A Very Small Chaotic Neural Net

Carlos Lourenço

***Abstract*— Previously we have shown that chaos can arise in networks of physically realistic neurons [1], [2]. Those networks contain a moderate to large number of units connected in a spatial arrangement providing instances of so-called Cellular Neural Networks. It was proposed that the flexibility and wide range of behaviors of chaos could be of computational value, namely in spatiotemporal regimes and when coupled with a chaos control process, either in biological or artificial nets. Here we aim to find a minimal network of realistic neurons already featuring a chaotic regime. Such a small network can be computationally useful per se, or otherwise constitute the building block of larger networks with even richer dynamical regimes. Our investigation unveils the role of the interplay between a homoclinic tangency and the presence of delays in neural signal transmission in the creation of complex behavior.**

I. Introduction

Chaos can be observed in neural networks even when realistic model neurons are considered [1], [2]. While careful exploration of parameter space is convenient, no purposeful mathematical gadgets need to be added in order to obtain complex behavior. Suggestions of the computational usefulness of chaos were given in [3], [4], [5], namely by showing how visual pattern processing can take place in biologically inspired networks [3], [5]. In previous work we focused on network properties requiring that a large enough number of neurons be connected in some spatial arrangement. In the present paper we downsize the network to as few as two units, actually one excitatory and one inhibitory neuron. We thus obtain a minimal chaotic building block. This can then be used either as a standalone complexity generator module or in the creation of larger networks where e.g. spatial symmetries can also be explored. The two latter applications, however, are outside the scope of this paper.

II. A minimal realistic model

We adopt a model of the leaky integrator type, endowed with time-delays in the signal transmission between neurons [6], [2]. Passive and active membrane properties are featured. Neuron connectivity is nonlinear, via the well-known sigmoidal activation function. Details of the model derivation can be found in [2]. Here we consider a simplified version which can be viewed as either modeling an excitatory neuron interacting with an inhibitory one, or otherwise representing the uniform activity of, respectively, a population of excitatory and inhibitory neurons coupled together. Individual neurons are not oscillators under the present model. However, oscillations in electrical activity arise due to the presence of excitatory and inhibitory feedback through synaptic connections.

Carlos Lourenço is with the Informatics Department, Faculty of Sciences, University of Lisbon, Campo Grande, 1749-016 Lisboa, Portugal, and with the Center for Logic and Computation, Department of Mathematics, IST, Av. Rovisco Pais, 1049-001 Lisboa, Portugal (phone: 351-217500601; fax: 351-217500084; email: csl@di.fc.ul.pt).

Mathematically, the model consists in a set of two coupled nonlinear delay differential equations,

$$\begin{aligned} \frac{dX}{dt} &= -\gamma(X - V_L) - (X - E_1)\,\Omega_1\,F_X[X(t-\tau)] \\ &\quad - (X - E_2)\,\Omega_2\,F_Y[Y(t-\tau)] \qquad (1) \\ \frac{dY}{dt} &= -\gamma(Y - V_L) - (Y - E_1)\,\Omega_3\,F_X[X(t-\tau)]\,. \end{aligned}$$

Here, X represents the membrane potential of an excitatory neuron, and Y that of an inhibitory neuron. The different equilibrium potentials have the values $V_L = -60$ mV, $E_1 = 50$ mV, and $E_2 = -80$ mV. As with other parameters of the model, these values are suggested by electrophysiological experiments [6], [7]. The inverse of the membrane's time-constant takes the value $\gamma = 0.25$ msec^{-1}. The sigmoidal activation function is of the form

$$F(V) = \frac{1}{1 + e^{-\alpha(V - V_c)}}\,.$$

The parameters α and V_c are adjusted so that the neuron is silent for a potential V lower than some activation threshold, and the firing rate saturates for a certain higher value of V. V_c is fixed at -25 mV, whereas $\alpha_X = 0.09$ mV^{-1} and $\alpha_Y = 0.2$ mV^{-1}. Note that there is a delay τ in signal transmission, including the case of the excitatory neuron feeding back onto itself. The delay is a varying parameter of the model. All types of connections are present except the inhibitory-to-inhibitory one. Synaptic weights are given by $\Omega_1 = 6.3$, $\Omega_2 = \Omega_3 = 5$ everywhere in this text except in Fig. 2 where Ω_2 is allowed to vary. From Eqs. (1), it is clear that, in the absence of coupling, the neurons would simply relax toward the V_L equilibrium. By this we refer to the case where the self-coupling of X, with delay τ, would also be absent. This would correspond to Eqs. (1) being left without any F_X or F_Y terms.

III. Route to chaos

By varying the parameters of system (1), a wide range of dynamical behaviors can be observed. To gain some analytical understanding of the system, one may keep most of the parameters fixed, and change the few remaining parameters. In this manner, one can identify the loci of bifurcations from steady states into other stationary states or into periodic oscillations. Such bifurcation diagrams have been calculated elsewhere [8], for typical sets of fixed parameters. Destexhe has also estimated the network size for which uniform oscillations of networks of neurons of the above type become linearly unstable [8]. However, that is a multi-unit scenario clearly different from the one we are considering. In our

case, bifurcations do lead to chaos and this happens for as few as two neurons. Let us note that different routes to chaos, namely of a spatiotemporal nature, are possible if we turn directly to the multi-unit case [8], [2].

To investigate the creation of oscillatory solutions, we considered Hopf bifurcations with different types of system parameters acting as the bifurcation parameter. These included the values of synaptic strengths Ω_I, of the propagation delay τ, and of the transfer functions' slopes α_X and α_Y.

Figure 1 provides an example of a Hopf bifurcation unfolded by varying τ in Eqs. (1).

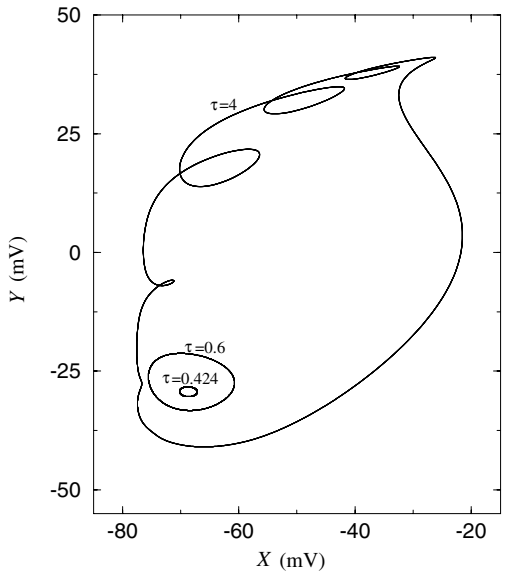

Fig. 1. Hopf bifurcation from a stationary solution of Eqs. (1). The amplitude of the cycles increases with the value of the time-delay τ. Apart from τ, all other parameters of Eqs. (1) are fixed and have the values as indicated in the main text.

Shown are three limit cycles obtained for different values of the delay[1]. The cycles with $\tau = 0.424$ and $\tau = 0.6$ are relatively close to the onset of the bifurcation. With $\tau = 4$, a solution with higher amplitude and more complex structure is seen. With the same fixed parameters as in this figure, for higher values of τ, chaotic solutions are observed. This is strong evidence that time-delays are of crucial importance in neuronal modeling, and can change completely the nature of the dynamics. For instance, with $\tau < 0.42$ and all other parameters as in Fig. 1, only a stationary state can be observed asymptotically.

It is known that dynamical systems may present different routes to chaos. In the following, we identify a possible route to chaotic behavior of Eqs. (1). For finite regions of the parameter-space, the system may present bursting oscillations. Figure 2 shows some examples of bursting regimes. In this figure, τ takes different values, and the synaptic weight Ω_2 is also allowed to vary from the usual value $\Omega_2 = 5$. The

[1]Since the full dynamics is infinite-dimensional due to the delay terms, the figure only displays projections of that dynamics on the (X, Y) space.

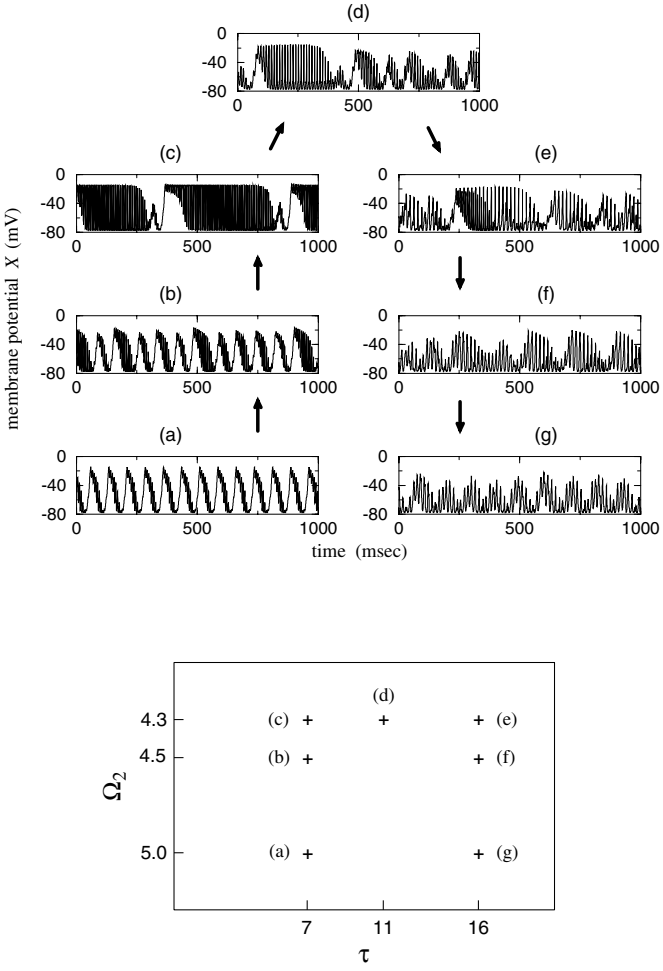

Fig. 2. **(a), (b)** and **(c)**: homoclinic tangency to an unstable limit cycle, with system (1). **(d)** to **(g)**: continuation of the sequence, showing a route to temporal chaos by destabilization of the regular sequence of bursts. The up-most part of the figure shows time-series of the membrane potential of the excitatory neuron, for different values of the parameters Ω_2 and τ. The latter are depicted in the down-most diagram. Arrows indicate one proposed route to chaos. Note that the time-series of (d) has been placed above those of (c) and (e) for readability reasons. Graphs (c), (d) and (e) actually share a common value $\Omega_2 = 4.3$. Apart from τ and Ω_2, the remaining parameters of Eqs. (1) are fixed. See text for details.

bursting oscillations are characterized by two different time-scales. Very fast oscillations are superimposed on a basic cycle occurring on a much longer time-scale. Following a suggestion by Gaspard (see also [9]), the bursting oscillations have been interpreted as signaling the presence of a homoclinic tangency to an unstable limit cycle [10]. The basic phenomenon concerns the graphs (a), (b) and (c) of Fig. 2, which are obtained with successively smaller values of Ω_2 and all other parameters fixed. As Ω_2 is decreased, the duration of the active phase, as well as the number of fast pseudo-cycles thereof, increase continuously. The intermediate segment, or silent phase, remains practically unchanged. For a critical value of Ω_2 close to 4.26, an infinite-period bifurcation takes place. Exactly at the bifurcation point, the bursting phase lasts an infinite time. For lower values of Ω_2 past that point,

the dynamics collapses into a stationary solution (not shown in the figure). At the bifurcation, the stationary solution is given by $(X, Y) = (-13.38\,,\ 43.04)$ mV. In analogy with the case studied by Destexhe and Gaspard [10], the following explanation can be proposed[2]. A limit cycle, called LC2, accounts for the fast oscillations. There is another cycle, LC1, which is born in a familiar way at a Hopf bifurcation[3] and which increases in amplitude (as Ω_2 is decreased) until it "collides" with LC2. LC2 cannot exist without the intermediate segment. Therefore, LC2 must be an unstable limit cycle. Let us consider the induced discrete-time dynamics at a Poincaré section transverse to the continuous-time cycles. LC2 appears to be a cycle of saddle type, because orbits like LC1 may enter the vicinity of LC2 along a path close to the stable manifold of LC2, and then escape along a path close to the unstable manifold of LC2. The bursting oscillations appear when LC1 grows to a point where it approaches significantly the region of phase-space where LC2 exists, such that the oscillations become increasingly LC2-like. Hence, the bursting can be interpreted as a transient distortion of the limit cycle LC1 due to the presence of LC2. At the critical point, or homoclinic tangency, LC1 coalesces with LC2. If viewed at the Poincaré section, the system's trajectory approaches the saddle fixed point LC2 exactly along the stable manifold of the latter, and escapes LC2 along its unstable manifold. At the bifurcation, the LC2-like oscillations are no longer a transient process, but last an infinite time. The exact homoclinic situation is inaccessible experimentally. Nonetheless, the approach of the critical situation is signaled by an increase of the bursts' duration, depending logarithmically on the distance to criticality [10]. This is illustrated as the sequence (a)→(b)→(c) of Fig. 2. In the previous investigation [10], the homoclinic tangency accounts for a succession of regular burst regimes akin to the one illustrated by that partial sequence of Fig. 2. Here, we extend the investigation by showing that irregular behavior of the chaotic type may also appear, associated with the homoclinicity. In Fig. 2, this corresponds *e.g.* to taking the system along a path in parameter-space given by the sequence (a)→ $\cdots$ →(g). This is one of the many possible sequences. For higher values of the delay τ, the succession of bursting periods gains an irregular character, until temporal chaos is obtained (for $\Omega_2 = 5$, in the figure). We propose therefore that chaos is associated with the interaction between the homoclinic tangency and the memory effect due to the presence of the delay terms[4]. Let us note that the role of homoclinic orbits in the generation of complex temporal behavior had been pointed out previously by several authors [11], [12].

In the remainder of the paper, we adopt the parameter values $\Omega_2 = 5$, $\tau = 16$ msec. The resulting chaotic regime is investigated for the system (1). In Figure 3, a Poincaré section of the dynamics of Eqs. (1) shows the lack of low-dimensional structure of the chaotic attractor.

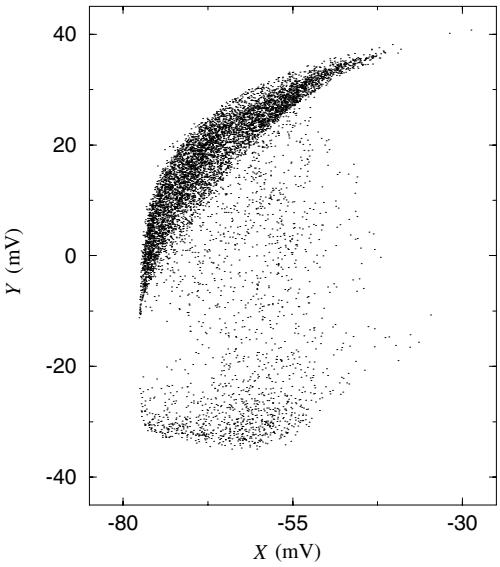

Fig. 3. Poincaré section obtained with Eqs. (1). $\Omega_2 = 5$, $\tau = 16$ msec, and the other parameters have the usual values. The figure is obtained by plotting the values $(X(t), Y(t))$ whenever $X(t - 4\ \text{msec}) = -35$ mV, $dX(t - 4\ \text{msec})/dt < 0$. There are 8368 points in the graph.

Figure 4 illustrates the same dynamics, but in continuous time. We also made a comparison of the above dynamics with that of a network comprising several chaotic neurons of the type described. Such comparison is not detailed in the present paper. Not surprisingly, we found that chaos is more developed in the full network case. Notwithstanding, by coupling several chaotic neurons we brought about a route to spatiotemporal chaos that had not yet been investigated by other authors. Indeed, the origin of spatiotemporal chaos in larger networks, in our case, is somewhat different from the one in [8], [13]. Given the route to chaos that we identified with the smaller system, Eqs. (1), we see that as few as two coupled neurons suffice to display chaotic behavior. Therefore, "spatiotemporal" chaos can be studied with arbitrarily small networks. We could thus study chaotic networks with between 2 and 32 neurons. References [8], [13] present a different picture. The Author's numerical simulations, with parameter values different from ours, show that uniform periodic oscillations of a network are destabilized only for network sizes greater or equal to $N_{\text{ex}} = 144$, $N_{\text{in}} = 36$, which are, respectively, the number of excitatory and inhibitory neurons. In the same numerical study, but with a less favorable connectivity pattern, the periodic bulk oscillations are not destabilized for network sizes smaller than $N_{\text{ex}} = N_{\text{in}} = 1600$. In the simulations in [8], [13], the destabilization of uniform solutions happens through a

[2]Those authors have not considered the same parameters as ours —hence they have not found chaos, but the homoclinic phenomenon is analogous.

[3]With τ fixed at 7 msec and all other parameters with the usual values, LC1 originates from a supercritical Hopf bifurcation of the fixed point $(X, Y) = (-75.53\,,\ -40.93)$ mV, at a critical value $\Omega_2 = 68.6$.

[4]Actually, the intermediate stages of the approach to the homoclinic tangency, at $\tau = 7$ msec, already show some irregularity. But chaos is only really developed for delay values greater than about 8 msec, and appropriate values of Ω_2.

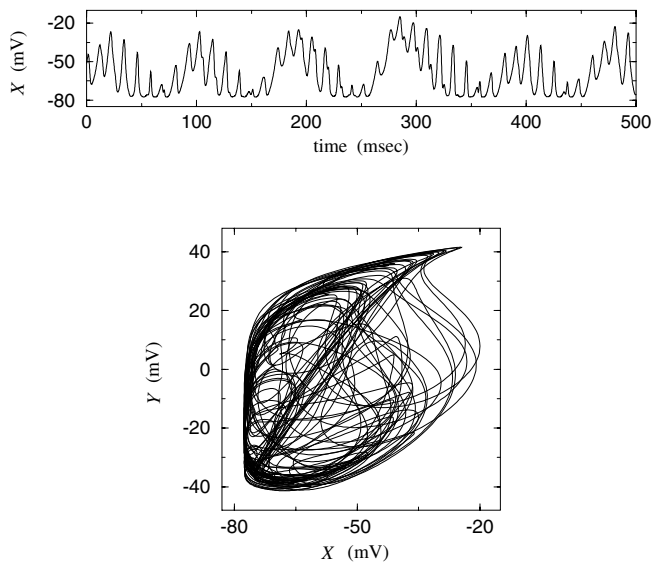

Fig. 4. **Top**: Chaotic time-series of the activity of the excitatory neuron in Eqs. (1). **Bottom**: Phase portrait of the system in the chaotic regime. Model parameters are as in Fig. 3.

type of spatiotemporal intermittency (see *e.g.* Figure 4 of Ref. [13]) that is not featured in our study of larger networks. The same Author shows theoretically that periodic bulk oscillations are destabilized for network sizes greater than $N_{\rm ex} = N_{\rm in} = 9$, but with special network configurations that we do not consider.

IV. Conclusions

We described a minimal network of realistic continuous-time neurons which are capable only of relaxing toward equilibrium when taken is isolation, but which display chaotic dynamics when synaptically coupled and in the presence of time-delays. Two neurons suffice to observe the chaotic behavior.

Although the paper's emphasis is on the dynamics of a very small network, we also pointed out that such small chaotic modules could be connected in order to obtain larger networks with more complex dynamical regimes. These include spatiotemporally chaotic regimes, albeit of a different nature from the ones investigated by other authors and also from the ones proposed in other studies by the present author [2].

Chaos may become most useful computationally when coupled with some form of chaos control [5]. Such control was achieved by us with the present model, both in the two-neuron version and for larger networks. While the discussion of a particular control procedure had already been provided [1], the actual mechanism of chaos generation in the homoclinic context is discussed only in the present paper.

Dynamical features of this biologically inspired model were revealed through theoretical considerations and numerical simulations. In subsequent work, an electronic implementation could be envisaged such that dynamical and computational properties might be explored in an actual physical device.

Acknowledgment

The author acknowledges the partial support of Fundação para a Ciência e a Tecnologia and EU FEDER via the Center for Logic and Computation and the project ConT-Comp (POCTI/MAT/45978/2002), and also via the project PDCT/MAT/57976/2004.

References

[1] C. Lourenço and A. Babloyantz, "Control of chaos in networks with delay: A model for synchronization of cortical tissue", *Neural Computation*, vol. 6, pp. 1141–1154, 1994.

[2] C. Lourenço, "Dynamical reservoir properties as network effects", *Proc. 14^{th} European Symposium on Artificial Neural Networks*, Bruges, Belgium, 26–28 April 2006 (in print).

[3] A. Babloyantz and C. Lourenço, "Computation with chaos: A paradigm for cortical activity", *Proceedings of the National Academy of Sciences USA*, vol. 91, pp. 9027–9031, 1994.

[4] N. Crook and T. Scheper, "A novel chaotic neural network architecture", *Proc. 9^{th} European Symposium on Artificial Neural Networks*, Bruges, Belgium, April 25–27, pp. 295–300, 2001.

[5] C. Lourenço, "Attention-locked computation with chaotic neural nets", *International Journal of Bifurcation and Chaos*, vol. 14, pp. 737–760, 2004.

[6] L. Kaczmarek, "A model of cell firing patterns during epileptic seizures", *Biological Cybernetics*, vol. 22, pp. 229–234, 1976.

[7] E. Kandel, J. Schwartz, and T. Jessell, Editors, *Principles of Neural Science*, New York, NY: McGraw-Hill Medical, 4th edition, 2000.

[8] A. Destexhe, Ph.D. Dissertation, Université Libre de Bruxelles, March 1992.

[9] P. Gaspard and X.-J. Wang, "Homoclinic orbits and mixed-mode oscillations in far-from-equilibrium systems", *Journal of Statistical Physics*, vol. 48, pp. 151–199, 1987.

[10] A. Destexhe and P. Gaspard, "Bursting oscillations from a homoclinic tangency in a time delay system", *Physics Letters A*, vol. 173, pp. 386–391, 1993.

[11] P. Gaspard and G. Nicolis, "What can we learn from homoclinic orbits in chaotic dynamics?", *Journal of Statistical Physics*, vol. 31, pp. 499–518, 1983.

[12] P. Glendinning and C. Sparrow, "Local and global behavior near homoclinic orbits", *Journal of Statistical Physics*, vol. 35, 645–696, 1984.

[13] A. Destexhe, "Oscillations, complex spatiotemporal behavior, and information transport in networks of excitatory and inhibitory neurons", *Physical Review E*, vol. 50, pp. 1594–1606, 1994.